Modeling traffic at sags

Goni Ros, B; Knoop, VL; Shiomi, Y; Takahashi, T; van Arem, B; Hoogendoorn, SP

DOI
10.1007/s13177-014-0102-3

Publication date
2016

Document Version
Accepted author manuscript

Published in
International Journal of Intelligent Transportation Systems Research

Modeling traffic at sags

Bernat Goñi Ros[a,*], **Victor L. Knoop**[a], **Yasuhiro Shiomi**[b], **Toshimichi Takahashi**[c], **Bart van Arem**[a], **Serge P. Hoogendoorn**[a]

[a] Department of Transport and Planning, Faculty of Civil Engineering and Geosciences, Delft University of Technology. Stevinweg 1, 2628 CN, Delft, The Netherlands.

[b] Department of Environmental Systems Engineering, College of Science and Engineering, Ritsumeikan University. 1-1-1 Nojihigashi, Kusatsu-shi, Shiga Prefecture 525-8577, Japan.

[c] Technical Centre, Toyota Motor Europe. Hoge Wei 33, B-1930, Zaventem, Belgium.

* Corresponding author. E-mail: b.goniros@tudelft.nl / Tel.: +31 152784912.

Abstract

Freeway capacity decreases at sags due to local changes in car-following behavior. Consequently, sags are often bottlenecks in freeway networks. This article presents a microscopic traffic model that reproduces traffic flow dynamics at sags. The traffic model includes a new car-following model that takes into account the influence of freeway gradient on vehicle acceleration. The face-validity of the traffic model is tested by means of a simulation study. The study site is a sag of a Japanese freeway. The simulation results are compared to empirical traffic data presented in previous studies. We show that the model is capable of reproducing the key traffic phenomena that cause the formation of congestion at sags, including the lower capacity compared to normal sections, the location of the bottleneck around the end of the vertical curve, and the capacity drop induced by congestion. Furthermore, a sensitivity analysis indicates that the traffic model is robust enough to reproduce those phenomena even if some inputs are modified to some extent. The sensitivity analysis also shows what parameters need to be calibrated more accurately for real world applications of the model.

Keywords

Sag, Traffic congestion, Microscopic traffic model, Model face-validity, Sensitivity analysis

1. Introduction

The *gradient* of a freeway is the inclination of the freeway surface to the horizontal. *Sags* or sag vertical curves are freeway sections along which the gradient increases gradually in the direction of traffic. The capacity of sags is generally lower than that of normal freeway sections [1, 2]. Consequently, sags often cause congestion in high traffic demand conditions [1]. The main reason why the freeway capacity decreases at sags is related to local changes in car-following behavior [3-7].

In order to evaluate the effectiveness of possible traffic management measures aimed at mitigating congestion at sags, it is necessary to be able to simulate traffic at that type of bottlenecks in a realistic way. This

paper presents a microscopic traffic model that reproduces traffic flow dynamics at sags. The model consists of two sub-models: a car-following model and a lane change model. The main novelty is the car-following modeling approach, which is based on assumptions about the way in which sags affect longitudinal driving behavior that are more realistic than those of existing models, and has a very generic formulation.

The face-validity of the traffic model is tested by means of a simulation study. The study site is the Yamato sag (Tomei Expressway, Japan). The traffic flow patterns obtained from simulation are compared to the patterns observed in empirical traffic data according to previous studies. Furthermore, we carry out a sensitivity analysis aimed at evaluating the robustness of the model to changes in key model inputs, and at determining the way in which modifying each of those model inputs influences the characteristics of the simulated traffic.

The rest of this article is structured as follows: Section 2 describes the main causes of congestion at sags according to the scientific literature; Section 3 specifies the requirements of the traffic model and analyzes the suitability of existing models; Section 4 presents the microscopic traffic model; Section 5 presents the methodology used to test the face-validity of the traffic model; Section 6 reports the results of the analysis; and Section 7 presents the conclusions of this study.

2. Causes of congestion at sags

Various empirical studies show that the capacity of sags is considerably lower than the capacity of normal sections (up to 30% lower) [1, 2]. Because of that, sags are often bottlenecks in freeway networks, hence they cause the formation of congestion in conditions of high traffic demand. In general, the bottleneck is located 500 to 1000 m downstream of the bottom of the sag [3]. The factors reducing the capacity of sags seem to be related primarily to two changes in car-following behavior that occur when vehicles go through the vertical curve: i) drivers tend to reduce speed [1, 3, 4]; and ii) drivers tend to keep longer headways than expected given their speed [5, 6, 7]. These changes in car-following behavior seem to be unintentional [6]. They are caused by a decrease in vehicle acceleration resulting from the combination of two factors: i) increase in resistance force; and ii) insufficient acceleration operation by drivers [1, 6]. Drivers fail to accelerate sufficiently even though they generally perceive the increase in slope [4, 6]. The reason why drivers do not accelerate sufficiently seems to be related to their throttle operation behavior: drivers generally push down the throttle pedal at the beginning of the vertical curve but it takes time for them to adjust the throttle position so as to fully compensate for the increase in resistance force [6]. Drivers are generally able to re-accelerate and recover their desired speed once they leave the vertical curve [3, 6].

Typically, in freeways with keep-left or keep-right rules, the process of congestion formation at sags consists of two phases. In the first phase, congestion forms on the median lane [1, 8, 9]. The main reason why congestion emerges first on the median lane is related to the characteristics of lane flow distribution: with high demand and uncongested traffic, flows tend to be higher (and closer to capacity) on the median lane than on the other lanes [8, 10]. In the second phase, congestion spreads from the median lane to the other lanes [1, 8, 9]. That process can be described as follows. When traffic becomes congested on the median lane, some vehicles migrate from that lane to the less crowded lanes in order to avoid queuing [8, 9]. When the flow on those lanes exceeds their capacity, traffic also breaks down there. At that point, traffic is congested on all lanes, which causes a

significant decrease in total outflow (due to the *capacity drop* phenomenon [11]) and the formation of a queue upstream of the bottleneck [1, 9].

3. Model requirements and suitability of existing models

As discussed in Section 2, the main traffic phenomena involved in the formation of congestion at sags are: a) decrease in vehicle acceleration and local changes in car-following behavior; b) low capacity of sags compared to normal sections (the bottleneck being the end of the vertical curve); c) congestion-induced capacity drop; d) queue dynamics; e) uneven lane flow distribution in high demand conditions; and f) migration of vehicles from congested to uncongested lanes. Any model that aims to reproduce traffic at sags in a realistic way should be capable of reproducing all the traffic phenomena mentioned above.

In order to reproduce phenomena e and f, the traffic model needs to include a lane change model. Note that there is no empirical evidence suggesting that lane-changing behavior is different at sags than in normal sections. For that reason, we conclude that it is sufficient to use a regular lane-change model, in which the set of variables that determine the decision to change lanes does not include the freeway gradient (it includes variables such as the difference in speed between lanes).

In order to reproduce phenomena a, b, c and d, the traffic model needs to include a car-following model. As discussed in Section 2, drivers significantly change their car-following behavior when they go through a sag, which is the main cause of the difference in capacity between sags and normal sections. Therefore, the car-following model needs to include the freeway gradient as separate variable in addition to the variables that determine regular car-following behavior (e.g., speed and distance to the preceding vehicle). Furthermore, the car-following model needs to adequately reproduce the influence of the freeway gradient on vehicle acceleration. Particularly, the model needs to reproduce: i) the limiting effect that an increase in gradient has on vehicle acceleration; ii) the inability of drivers to fully compensate for that limiting effect immediately; iii) the resulting changes in car-following behavior at sags (i.e., speed reduction and increase in headways); and iv) the creation of a capacity bottleneck at the end of sag vertical curves. In addition, the car-following model also needs to reproduce the ability of drivers to gradually regain their normal car-following behavior once they leave the vertical curve.

Several car-following models have been developed in the last decades with the objective of reproducing longitudinal driving behavior at sags. Those models can be grouped into two broad categories based on whether they assume that drivers do or do not explicitly compensate for the limiting effect that an increase in freeway gradient has on vehicle acceleration. Examples of models that assume no explicit compensation are those proposed by Koshi *et al.* [1] and Komada *et al.* [12]. Both models assume that a constant positive slope has a constant negative influence on vehicle acceleration. However, that assumption is not consistent with empirical observations, which show that drivers generally regain their normal car-following behavior as they climb an uphill section (at least if the uphill section is not too steep) [3, 6].

Examples of models that assume that drivers explicitly compensate for the limiting effect that an increase in gradient has on vehicle acceleration are those proposed by Yokota *et al.* [13] and Oguchi & Konuma [14]. Yokota *et al.* [13] present a car-following model that assumes that drivers are able to fully compensate for

changes in gradient with a certain time delay. Hence a constant slope has a decreasing influence on vehicle acceleration. This is more in line with empirical observations. However, an important disadvantage of that model is that it does not accurately reproduce the location of the bottleneck at sags. The model generates a bottleneck around the bottom of the sag [13], whereas empirical observations show that the bottleneck is generally located around the end of the vertical curve [3, 9].

Oguchi & Konuma [14] present a model that assumes that drivers compensate for the increase in resistance force caused by an increase in freeway gradient in such a way that the sensitivity of the vehicle acceleration to that increase in resistance force decreases over time as the vehicle moves along the vertical curve and the subsequent uphill section. The authors show that their model reproduces the car-following behavior of drivers (as observed in a driving simulator environment) better than models assuming that drivers do not explicitly compensate for the limiting effect that an increase in gradient has on vehicle acceleration [14]. Oguchi & Konuma do not present simulated traffic data, but one may expect that with appropriate parameter values their model generates a bottleneck at the end of sag vertical curves, which is the location where the limitation on vehicle acceleration caused by the gradient term is stronger. However, one drawback of the model proposed by Oguchi & Konuma [14] is that it is not sufficiently generic. More specifically, the values of some parameters (such as T_a and T_W) necessarily depend on the vertical profile of the sag.

We conclude that in order to model traffic at sags, it is sufficient to use a regular lane change model, but it is necessary to develop a new car-following model. That model should reproduce the characteristics of car-following behavior at sags and their effect on freeway capacity in a realistic way. To that end, the main principle of the modeling approach proposed by Oguchi & Konuma [14] seems adequate. However, that principle should be re-formulated in such a way that the model parameters are independent of the vertical profile of the freeway, in order to make the model generic for all sags.

4. Microscopic traffic model

The proposed microscopic traffic model consists of two sub-models: i) a car-following model; and ii) a lane change model. The two sub-models are presented in Section 4.1 and Section 4.2, respectively. The inputs required by the traffic model are described in Section 4.3.

4.1. Car-following model

We developed a new car-following model that takes into account the influence of vertical curves on vehicle acceleration. The model determines the vehicle acceleration by means of a two-term additive function:

$$\dot{v}(t) = f_{\mathrm{r}}(t) + f_{\mathrm{g}}(t) \tag{1}$$

The first term in Eq. 1 (f_r) describes regular car-following behavior. Its formulation is based on the Intelligent Driver Model (IDM) [15]. This term accounts for the influence of speed (v), relative speed (Δv) and spacing (s) on vehicle acceleration:

$$f_r(t) = a \cdot \left[1 - \left(\frac{v(t)}{v_{des}} \right)^4 - \left(\frac{s_{des}\left(v(t), \Delta v(t)\right)}{s(t)} \right)^2 \right] \quad (2)$$

where the dynamic desired spacing (s_{des}) is:

$$s_{des}\left(v(t), \Delta v(t)\right) = s_s + v(t) \cdot T\left(v(t)\right) + \frac{v(t) \cdot \Delta v(t)}{2\sqrt{a \cdot b}} \quad (3)$$

and the safe time headway (T) depends on the traffic state:

$$T\left(v(t)\right) = \begin{cases} T_F & \text{if } v(t) \geq v_{crit} \\ \gamma \cdot T_F & \text{if } v(t) < v_{crit} \end{cases} \quad (4)$$

The parameters in Eq. 2-4 are: desired speed (v_{des}); maximum acceleration (a); maximum comfortable deceleration (b); net spacing at standstill (s_s); safe time headway in uncongested traffic conditions (T_F); congestion factor on safe time headway ($\gamma > 1$); and critical speed (v_{crit}). The critical speed is used as threshold to differentiate between congested and uncongested traffic.

The second term in Eq. 1 (f_g) accounts for the influence of vertical curves on vehicle acceleration. At a given time t, that influence is the difference between the gradient at the location where the vehicle is at that time ($G(x(t))$) and the gradient compensated by the driver until that time ($G_c(t)$), multiplied by a sensitivity parameter (θ):

$$f_g(t) = -\theta \cdot \left[G\left(x(t)\right) - G_c(t) \right] \quad (5)$$

The compensated gradient (G_c) is a variable that accounts for the fact that drivers have a limited ability to compensate for the negative effect that an increase in gradient has on vehicle acceleration. The model assumes that drivers compensate for any increase in freeway gradient linearly over time with a maximum gradient compensation rate defined by parameter c. The value of parameter c does not depend on the vertical profile of the sag. This assumption is based on findings by Yoshizawa *et al.* [6], who found that, when drivers go through a sag, they push down the throttle pedal at a similar rate regardless of the vertical profile of the sag. Note that the model assumes that drivers are able to fully compensate for any decrease in gradient (e.g., at crest vertical curves) immediately. Therefore, the compensated gradient at a given time t is defined as follows:

$$G_c(t) = \begin{cases} G\left(x(t)\right) & \text{if } G\left(x(t)\right) \leq G(t_c) + c \cdot (t - t_c) \\ G(t_c) + c \cdot (t - t_c) & \text{if } G\left(x(t)\right) > G(t_c) + c \cdot (t - t_c) \end{cases} \quad (6)$$

where t_c is the time when the driver could no longer fully compensate for the gradient change:

$$t_c = \max\left(t \mid G_c(t) = G\left(x(t)\right)\right) \quad (7)$$

The properties of the model are as follows. If the gradient profile of a sag is such that the rate at which the freeway gradient increases is lower than the driver's maximum gradient compensation rate (c), then $G - G_c = 0$ (hence $f_g = 0$) at any time t. Consequently, at very gentle sags, the increase in freeway gradient has no effect on

vehicle acceleration, so acceleration is determined only by the regular car-following behavior term (f_r). However, at sags where the rate at which the gradient increases is higher than the driver's maximum gradient compensation rate (c), then $G - G_c > 0$ for a certain period of time. During that period, the compensated gradient (G_c) increases linearly over time but f_g is negative, which limits vehicle acceleration. It is important to remark two things about the latter type of sags. First, the sharper the sag, the greater the value of $G - G_c$ along the sag, hence the stronger the vehicle acceleration limitation. Second, of all locations along the freeway, vehicle acceleration limitation is maximum at the location where the gradient increase rate becomes lower than the driver's maximum gradient compensation rate (i.e., the end of the sag vertical curve), because $G - G_c$ is maximum at that location.

Note that the formulation of the second term of Eq. 1 (f_g) is based on a similar principle to that of the gradient term of the model presented by Oguchi & Konuma [14]. However, in our model, the values of the parameters of the gradient term (i.e., c and θ) do not necessarily depend on the vertical profile of the freeway. This makes our model more generic than the model presented by Oguchi & Konuma.

4.2. Lane change model

To model lane-changing behavior we used the Lane Change Model with Relaxation and Synchronization (LMRS) [16]. Note that we modified the LMRS with regard to the calculation of the speed gain desire incentive: in our model, the speed of all preceding vehicles that are not farther ahead than x_0 meters has the same weight in calculating the anticipated speed of downstream traffic. This modification allows drivers to anticipate more accurately the speed of downstream traffic when they drive into a queue and they have to decide whether to change lanes.

4.3. Model inputs

The traffic model requires the user to provide the following inputs: i) simulation period; ii) characteristics of the freeway; iii) traffic demand profile; and iv) traffic composition. The freeway characteristics include length, number of lanes, vertical profile (i.e., degree of gradient over distance) and speed limits. The traffic demand profile specifies the flow entering the simulated freeway stretch over time (per lane). The traffic composition describes the characteristics of the vehicle-driver units that enter the freeway. The vehicle characteristics taken into account by the model are vehicle type (passenger car, truck, etc.) and vehicle length (l). The driver characteristics are the parameters of the car-following model and the lane change model.

5. Model verification methodology

The face-validity of the traffic model described in Section 4 was tested by means of a simulation study. The objective was to determine the model's ability to realistically reproduce traffic flow dynamics at sags. First, we defined a freeway stretch containing a sag and we simulated traffic using our traffic model. We analyzed the traffic flow patterns obtained from simulation and we compared them with the patterns observed in empirical data. Second, we performed a sensitivity analysis. The objectives of that analysis were to determine: i) the

robustness of the model to changes in key model inputs; and ii) the way in which modifying each of those model inputs influences the simulation results. The general simulation setup is presented in Section 5.1. The scenarios of the sensitivity analysis are defined in Section 5.2. Finally, Section 5.3 describes the indicators used to analyze the simulation results.

5.1. Simulation setup

Freeway characteristics. The simulated freeway stretch is 10 km long and has three lanes (median, center and shoulder). Vehicles enter the freeway at location $x = 0$; the exit point is at location $x = 10$ km. The freeway stretch has three sections: i) constant-gradient downhill section; ii) sag vertical curve; and iii) constant-gradient uphill section. The first and third sections have a constant gradient equal to -0.5% and 2.5%, respectively. The vertical profile of the sag is equivalent to that of the Yamato sag (Tomei Expressway, Japan): the gradient increases linearly from -0.5% to +2.5%, and the length of the vertical curve is 600 m (see Figure 1). The constant-gradient downhill section is long enough to ensure that if congestion forms at the sag, the queue does not spill back to the freeway entry point. The speed limit is 100 km/h for cars and 85 km/h for trucks on the whole freeway stretch. There are no on-ramps, off-ramps, lane drops or horizontal curves.

Simulation period and traffic demand profile. The simulation period is 100 min. The total traffic demand (on all lanes) increases linearly from 3000 to 5200 veh/h between $t = 0$ and $t = 75$ min. From $t = 75$ min to $t = 100$ min, the total inflow stays at 5200 veh/h. Given the total demand, the demand per lane was defined based on a lane flow distribution model presented by Wu [17]. We used the same parameter values provided in reference [17] for three-lane freeways (see Table 6 of that reference), except for a and e on the center lane (we used $a = 0.39$ and $e = 0.30$). We slightly modified the values of those two parameters to make the lane flow distribution model more accurate for Japanese freeways, based on empirical data presented by Xing *et al.* [10]. Note that after entering the freeway, vehicles are free to change lanes in accordance with the lane change model.

Traffic composition. We defined two types of vehicles (cars and trucks), which have different vehicle length (4 and 15 m, respectively). Furthermore, we defined three types of car drivers (each corresponding to one lane) and one type of truck driver. Defining one type of car driver per lane was necessary to take into account the differences in desired speed and target time headway between lanes observed in empirical traffic data [9]. The parameters of the car-following model and the lane change model are different for each driver type (see Table 1). For the interpretation of the lane change model parameters, we refer to reference [16]. Table 2 shows the percentage of vehicles entering the freeway on each lane that belong to each vehicle and driver type. Note that we defined some parameters of the car-following model and the lane change model as stochastic parameters (v_{des}, a, b, T_F, c, T_{min} for car drivers, and v_{des} for truck drivers). The value of those parameters differs between drivers belonging to the same driver type. For car drivers, those parameters depend on the stochastic factor δ, which differs between drivers (it is normally distributed with mean δ^* and standard deviation σ_δ): $v_{des} = \delta \cdot v_{des,0}$; $a = \delta \cdot a_0$; $b = \delta \cdot b_0$; $T_F = T_{F,0}/\delta$; $c = \delta \cdot c_0$; and $T_{min} = T_{min,0}/\delta$. Note that the factor δ is defined per driver, hence all stochastic parameters corresponding to a particular driver are correlated. For trucks, only the desired speed

parameter is stochastic. That parameter is assumed to be normally distributed with mean $v^*_{des,t}$ and standard deviation $\sigma_{vdes,t}$.

Data collection system. We placed virtual loop detectors every 100 m all along the freeway stretch, on all lanes. Those detectors measure flow and average speed. The data aggregation period is 30 s.

5.2. Sensitivity analysis

To perform the sensitivity analysis, we defined a base scenario and several alternative scenarios. In the base scenario, the model inputs are those defined in Section 5.1. In the alternative scenarios, the model inputs are the same as in the base scenario, except for one of them, which is changed by a certain percentage. The modified inputs are the vertical curve length (L), the maximum gradient compensation rate (c_0), the congestion factor on target time headway (γ), and the sensitivity to the difference between gradient and compensated gradient (θ) (see Table 3). Note that we also defined a reference scenario, in which it is assumed that the sag vertical curve has no influence whatsoever on the acceleration behavior of drivers (i.e., $f_g(t) = 0$ at any time t). That hypothetical behavior is modeled by setting the value of the maximum gradient compensation rate parameter to a very high value (c_0 = 999 s^{-1}), leaving the other model inputs as in the base scenario. The reference scenario is used as input to analyze the traffic data obtained from simulation (see Section 5.3). Five simulation replications were carried out for each scenario.

5.3. Indicators

The key characteristics of the traffic flow patterns obtained from simulation were determined by analyzing the flow and speed data collected by the virtual loop detectors. To analyze the data, we used three main indicators: a) time-to-breakdown (TTBD); b) average exit flow after breakdown (s_{cong}); and c) average vehicle delay after breakdown (AVD_{cong}).

The time-to-breakdown (TTBD) is the time when traffic becomes congested at the end of the sag vertical curve on a lane and this is followed by the formation of persistent congestion on the other lanes as well (see, for example, Figures 2 and 3). As mentioned in Section 4.1, we consider that traffic becomes congested when the traffic speed goes below a certain threshold (v_{crit}). The speeds used to calculate the TTBD are those measured by the three virtual detectors (one on each lane) located at x = 8.2 km (i.e., near the end of the sag vertical curve).

The average total exit flow after breakdown (s_{cong}) is the average of the total exit flows measured from the time when traffic breaks down (i.e., TTBD) to the end of the simulation period. The total exit flow in a given aggregation period is defined as the sum of the flows measured by the three virtual detectors (one on each lane) located at x = 9.9 km (i.e., near the freeway exit point) during that period. The s_{cong} can be used as an estimate of the queue discharge capacity of the bottleneck.

The average vehicle delay after breakdown (AVD_{cong}) is calculated as follows:

$$\mathrm{AVD}_{\mathrm{cong}} = \frac{\mathrm{TTS}_{\mathrm{cong}} - \mathrm{TTS}_{\mathrm{ref}}}{N_{d,\mathrm{cong}}} \tag{8}$$

where: $\mathrm{TTS}_{\mathrm{cong}}$ is the total time spent by vehicles in the freeway stretch between the time when traffic breaks down (i.e., TTBD) and the end of the simulation period in a given scenario; $\mathrm{TTS}_{\mathrm{ref}}$ is the total time spent by vehicles in the freeway stretch in the reference scenario during the same time period used to calculate $\mathrm{TTS}_{\mathrm{cong}}$; and $N_{d,\mathrm{cong}}$ is the number of vehicles that enter the freeway during the time period used to calculate $\mathrm{TTS}_{\mathrm{cong}}$. Note that $N_{d,\mathrm{cong}}$ is the same in the target scenario and the reference scenario for each simulation replication.

In Eq. 8, the total time spent is calculated based on the total demand and exit flows using the method described in reference [18]. The total demand flow is defined as the sum of the flows measured by the three virtual detectors (one on each lane) located at x = 0.1 km. As mentioned above, the total exit flow is defined as the sum of the flows measured by the three virtual detectors (one on each lane) located at x = 9.9 km.

Finally, note that the values of the three indicators described above are expected to be different in different replications of the same scenario, because some parameters of the car-following and lane change models are stochastic (see Section 5.1). Therefore, the behavior of driver-vehicle units is not exactly the same in all replications of the same scenario, which influences both the demand profile and the capacity of the bottleneck.

6. Results

This section presents the results of the simulation study aimed at testing the face-validity of the traffic model. Section 6.1 analyzes the main characteristics of the traffic flow patterns obtained from simulation. Section 6.2 presents the results of the sensitivity analysis.

6.1. Simulated traffic flow patterns

In Figures 2 and 3, we can observe a typical example of the traffic flow patterns generated by the model. Those figures show flow and speed data corresponding to one of the base scenario simulation replications. In that simulation replication, traffic breaks down at t = 84 min (see Figures 2 and 3a), when total demand is 5200 veh/h. The bottleneck is the end of the sag vertical curve (see Figure 2).

The process of congestion formation is as follows: 1) traffic becomes congested on the median lane (see Figures 2 and 3a); 2) some drivers move out of the median lane, which causes a temporary increase in flow on the center and shoulder lanes (see Figure 3b); and 3) the capacity of the center and shoulder lanes is exceeded and traffic becomes congested there as well (see Figures 2 and 3a). Note that the migration of vehicles from the median lane to the other lanes causes a temporary decrease in flow on the median lane (see Figure 3b). That decrease in flow causes the queue on that lane to dissolve; however, the decrease in flow is only temporary, so traffic becomes congested on the median lane again a few minutes later (see Figures 2 and 3a).

The occurrence of congestion on a lane results in decreased lane flow (see Figure 3b). The average total exit flow after breakdown (which is an estimation of the queue discharge capacity of the bottleneck) is about 5000

veh/h, i.e., 4% lower than the total demand (see Figure 3c). As a result, after traffic breaks down, a queue of vehicles forms upstream of the bottleneck (see Figure 2), which leads to increased travel times (the average vehicle delay after breakdown is 13.6 s).

In conclusion, the traffic flow patterns obtained from simulation are similar to the patterns observed in real freeways. The traffic model is capable of reproducing the main phenomena that cause the formation of congestion at sags. The model generates a capacity bottleneck and reproduces its location quite accurately (i.e., end of the sag vertical curve), although the simulated free flow capacity (5200 veh/h) is lower than in empirical traffic data from the Yamato sag (5400 veh/h) [9]. In addition, the model reproduces the congestion-induced capacity drop, although the magnitude of the drop (4%) is lower than in empirical observations (11%) [9]. The model also reproduces the process of congestion formation [1, 8, 9]: congestion starts on the median lane and spreads to the other lanes as a result of lane changes. However, the frequency of lane changes from congested to uncongested lanes may be higher than observed in empirical data.

6.2. Sensitivity analysis

The results of the sensitivity analysis show that, in all replications of all scenarios: i) traffic breaks down at the sag, which indicates that the capacity of the sag is lower than that of the constant-gradient downhill section; ii) the head of the queue stays around the end of the vertical curve; and iii) congestion causes considerable travel time delays. However, there are notable differences between scenarios, which means that changing the values of L, c_0, θ and γ has an impact on the characteristics of the simulated traffic.

For instance, increasing the length of the vertical curve (L) generally leads to a slightly longer time-to-breakdown (i.e., traffic breaks down a bit later, as shown in Figure 4) and a higher queue discharge rate (Figure 5). Consequently, it also results in a lower average vehicle delay after breakdown (Figure 6). Increasing the maximum gradient compensation rate (c_0) has a similar effect to that of increasing the length of the vertical curve (see Figures 4-6). Instead, increasing the parameter θ (i.e., the sensitivity to the difference between gradient and compensated gradient) has the opposite effect: a higher θ generally results in a slightly shorter time-to-breakdown and a lower queue discharge rate, which causes an increase in AVD_{cong}. Those findings can be explained as follows. A longer L (hence a more gentle vertical curve), a greater c_0 (hence a faster compensation of the increase in freeway gradient by drivers) and a lower sensitivity to the difference between gradient and compensated gradient (θ) reduce the negative effect that the increase in freeway gradient has on vehicle acceleration (see Equations 5-7), which is the main cause of the changes in car-following behavior that reduce the capacity of the sag (see Section 2). As a result, congestion starts later in time and the queue discharge rate increases. Therefore, the average queue length within the simulation period decreases and the traffic speed within the queue increases, which leads to decreased AVD_{cong}.

The value of the congestion factor on target time headway (γ) influences traffic flow dynamics in a different way than the value of L, c_0 and θ. First, as shown in Figure 4, changing the value of parameter γ by -10%, -5% or +5% in comparison to the base scenario does not have any clear effect on the time-to-breakdown (Figure 4). However, if the value of parameter γ is increased by +10%, congestion starts considerably earlier (around 7 min earlier on average). Second, increasing the value of parameter γ generally leads to a lower queue discharge rate

(see Figure 5). As a consequence of the decreased queue discharge rate (and the unchanged or shorter time-to-breakdown), increasing the value of parameter γ results in higher average vehicle delay after breakdown (see Figure 6). Those findings can be explained as follows. A higher γ means longer headways in congestion; therefore, increasing the value of γ reduces the queue discharge capacity of the sag, which results in increased average vehicle delay after breakdown. However, increasing the value of parameter γ has little influence on the time when congestion starts. The average time-to-breakdown is only significantly different when γ is 10% higher than in the base scenario. The reason why this occurs is as follows. In the other scenarios, some slow-speed regions appear near the end of the vertical curve before traffic breaks down (see, for instance, Figure 2). Those slow-speed regions dissolve before they cause a full traffic breakdown because the inflow is lower than the outflow. However, increasing the value of parameter γ decreases the outflow from those low-speed regions, which in some cases prevents its dissolution. As a result, the slow-speed regions cause a full breakdown earlier than in the scenarios with lower value of γ. It is important to remark that the magnitude of the decrease in queue discharge rate caused by increasing the value of parameter γ is more pronounced than the magnitude of the decrease in queue discharge rate caused by increasing the value of θ or decreasing the value of L and c_0 (see Figure 5). Consequently, the magnitude of the increase in AVD_{cong} caused by increasing the value of parameter γ is also more pronounced than the magnitude of the increase in AVD_{cong} caused by increasing parameter θ or decreasing parameters L and c_0 (see Figure 6).

Finally, note that the time-to-breakdown differs substantially between simulation replications belonging to the same scenario, whereas the variation of the average exit flow after breakdown (s_{cong}) is much lower. As seen in Figures 4 and 5, the average standard deviation of the time-to-breakdown in all scenarios is around 8% of the mean (7 min), whereas the average standard deviation of s_{cong} in all scenarios is around 0.5% of the mean (30 veh/h). From this we conclude that the variation of the AVD_{cong} within each scenario is mainly due to the variation in the time-to-breakdown.

To sum up, the results of the sensitivity analysis show that the traffic model is capable of reproducing the main characteristics of traffic flow dynamics at sags even if some model inputs are modified to some degree. This indicates that the model is quite robust. However, modifying those inputs does have an influence on the characteristics of the simulated traffic, which stresses the need to calibrate and validate the traffic model. Changing the value of L, c_0, θ and γ influences traffic as follows. Congestion tends to start a bit earlier and be more severe if: i) the sag vertical curve is sharper (shorter L); ii) drivers compensate more slowly for the increase in freeway gradient (lower c_0); iii) vehicle acceleration is more sensitive to the difference between gradient and compensated gradient (higher θ); or iv) drivers keep longer time headways in congestion (higher γ). It is important to remark that changing the value of parameter γ has a larger effect on the characteristics of the simulated traffic (particularly on the queue discharge capacity) than changing the values of L, c_0 and θ by the same percentage (at least in the scenarios included in the analysis). This indicates that parameter γ should be given especial attention during the model calibration/validation process. Finally, the results of the sensitivity analysis also show that the stochasticity incorporated into the traffic model (see Section 5.1) has a strong influence on the time when congestion starts, whereas its influence on the queue discharge capacity of the bottleneck is less significant.

7. Conclusions

This paper presented a microscopic model that reproduces traffic flow dynamics at sags. The traffic model consists of two sub-models: i) a car-following model; and ii) a lane change model. The main novelty is the car-following modeling approach. We propose a new car-following model that is based on assumptions about the way in which sag vertical curves affect longitudinal driving behavior that are more realistic than those of most existing models. Our car-following model is based on a similar principle to that of the model presented by Oguchi & Konuma [14], which assumes that drivers compensate gradually for the increase in resistance force caused by an increase in freeway gradient. However, our car-following model has a more generic formulation.

The face-validity of the traffic model was tested by means of a simulation study. The traffic flow patterns obtained from simulation are similar to the patterns observed on real freeways. More specifically, the proposed traffic model is capable of reproducing the main traffic phenomena that cause the formation of congestion at sags, namely: a) decrease in vehicle acceleration and local changes in car-following behavior; b) low capacity of sags compared to normal sections (the bottleneck being the end of the vertical curve); c) congestion-induced capacity drop; d) queue dynamics; e) uneven distribution of flow across lanes in high demand conditions; and f) migration of vehicles from congested to uncongested lanes.

A sensitivity analysis indicates that the traffic model is sufficiently robust to reproduce those phenomena even if some model inputs are modified to some degree. However, modifying those inputs does have an influence on the characteristics of the simulated traffic (particularly on the queue discharge capacity of the bottleneck), which highlights the need to calibrate and validate the proposed traffic model. Parameter γ should be given especial attention in the calibration/validation process. The results of the sensitivity analysis also indicate potential ways to improve traffic flow efficiency at sags. For instance, the severity of congestion seems to be lower if the vertical curve is more gentle and if drivers are able to compensate faster for the negative effect that the increase in freeway gradient has on vehicle acceleration.

The calibration and validation of the traffic model will require a quantitative comparison of the model output with empirical traffic data. Vehicle trajectory data from the Yamato sag (Tomei Expressway, Japan) are available (see reference [7]). However, data from additional sites will also be necessary. If possible, those additional sites should be from other countries and include sags with different vertical profiles and different number of lanes. After calibration and validation, the model could be used to evaluate the effectiveness of possible control measures to mitigate congestion at sags.

Acknowledgments

This research was sponsored by Toyota Motor Europe. The authors would like to thank the anonymous reviewers for their valuable comments and suggestions to improve the quality of the paper.

References

[1] Koshi, M., Kuwahara, M., Akahane, H.: Capacity of sags and tunnels on Japanese motorways. ITE Journal

62(5), 17–22 (1992).

[2] Okamura, H., Watanabe, S., Watanabe, T.: “An empirical study on the capacity of bottlenecks on the basic suburban expressway sections in Japan”, Proceedings of the 4th International Symposium on Highway Capacity, Maui, Hawaii (2000).

[3] Brilon, W., Bressler, A.: Traffic flow on freeway upgrades. Transp. Res. Rec. **1883**, 112–121 (2004).

[4] Furuichi, T., Yamamoto, S., Kotani, M., Iwasaki, M.: “Characteristics of spatial speed change at motorway sag sections and capacity bottlenecks”, Proceedings of the 82nd Annual Meeting of the Transportation Research Board, Washington, D.C. (2003).

[5] Koshi, M.: An Interpretation of a Traffic Engineer on Vehicular Traffic Flow. In Fukui, M., Sugiyama, Y., Schreckenberg, M., Wolf, D.E. (eds.): Traffic and Granular Flow’01, Springer, Berlin, 199–210 (2003).

[6] Yoshizawa, R., Shiomi, Y., Uno, N., Iida, K., Yamaguchi, M.: Analysis of Car-following Behavior on Sag and Curve Sections at Intercity Expressways with Driving Simulator. Int. J. Intel. Trans. Sys. Res. **10**(2), 56–65 (2012).

[7] Goñi Ros, B., Knoop, V. L., van Arem, B., Hoogendoorn, S. P.: Empirical analysis of the causes of stop-and-go waves at sags. IET Intell. Transp. Syst. **8**(5), 499–506 (2014).

[8] Hatakenaka, H., Hirasawa, T., Yamada, K., Yamada, H., Katayama, Y., Maeda, M.: “Development of AHS for traffic congestion in sag sections”, Proceedings of the 13th ITS World Congress, London, U.K. (2006).

[9] Patire, A. D., Cassidy, M. J.: Lane changing patterns of bane and benefit: Observations of an uphill expressway. Transp. Res. B **45**(4), 656–666 (2011).

[10] Xing, J., Sagae, K., Muramatsu, E.: “Balance lane use of traffic to mitigate motorway traffic congestion with roadside variable message signs”, Proceedings of 17th ITS World Congress, Busan, South Korea (2010).

[11] Hall, F. L., Agyemang-Duah, K.: Freeway Capacity Drop and the Definition of Capacity. Transp. Res. Rec. **1320**, 91–98 (1991).

[12] Komada, K., Masukura, S., Nagatani, T.: Effect of gravitational force upon traffic flow with gradients. Phys. A **388**, 2880–2894 (2009).

[13] Yokota, T., Kuwahara, M., Ozaki, H.: “A study of AHS effects on traffic flow at bottlenecks”, Proceedings of the 5th ITS World Congress, Seoul, South Korea (1998).

[14] Oguchi, T., Konuma, R.: “Comparative study of car-following models for describing breakdown phenomena at sags”, Proceedings of the 19th ITS World Congress, Stockholm, Sweden (2009).

[15] Treiber, M., Hennecke, A., Helbing, D.: Congested traffic states in empirical observations and microscopic simulations. Phys. Rev. E **62**(2), 1805–1824 (2000).

[16] Schakel, W., Knoop, V. L., van Arem, B.: Integrated Lane Change Model with Relaxation and Synchronization. Transp. Res. Rec. **2316**, 47–57 (2012).

[17] Wu, N.: Equilibrium of lane flow distribution on motorways. Transp. Res. Rec. **1965**, 48–59 (2006).

[18] Papageorgiou, M., Diakaki, C., Dinopoulou, V., Kotsialos, A., Wang, Y.: Review of road traffic control strategies. Proceedings of the IEEE **91**, 2043–2067 (2003).

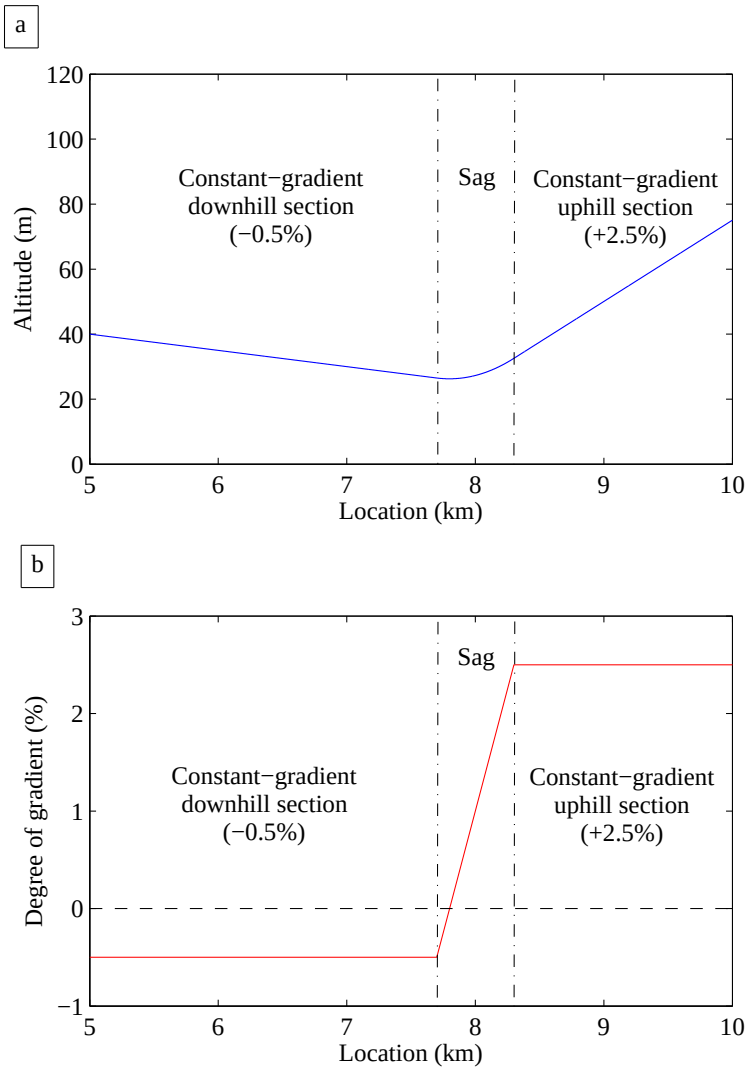

Figure 1. Vertical profile of the freeway stretch: a) altitude over distance; and b) gradient over distance.

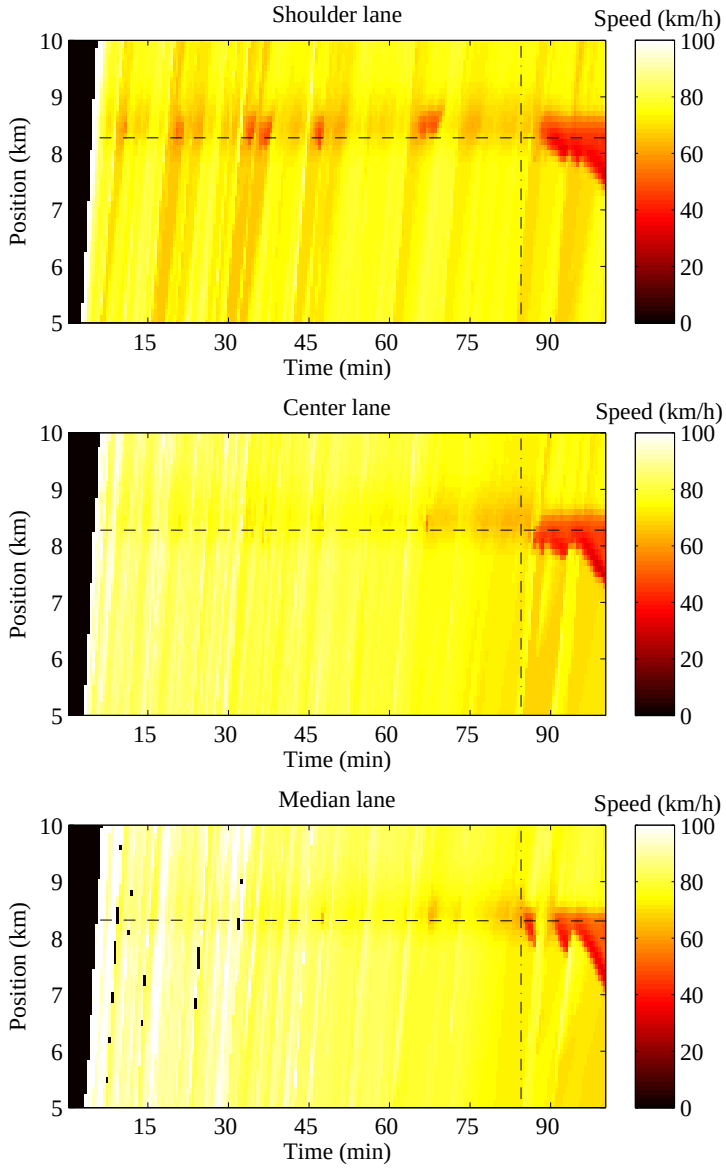

Figure 2. Speed contour plots of the shoulder lane, the center lane and the median lane in the base scenario (first simulation replication). The dash-dotted lines show the time-to-breakdown (TTBD), and the dashed lines indicate the location where the sag vertical curve ends.

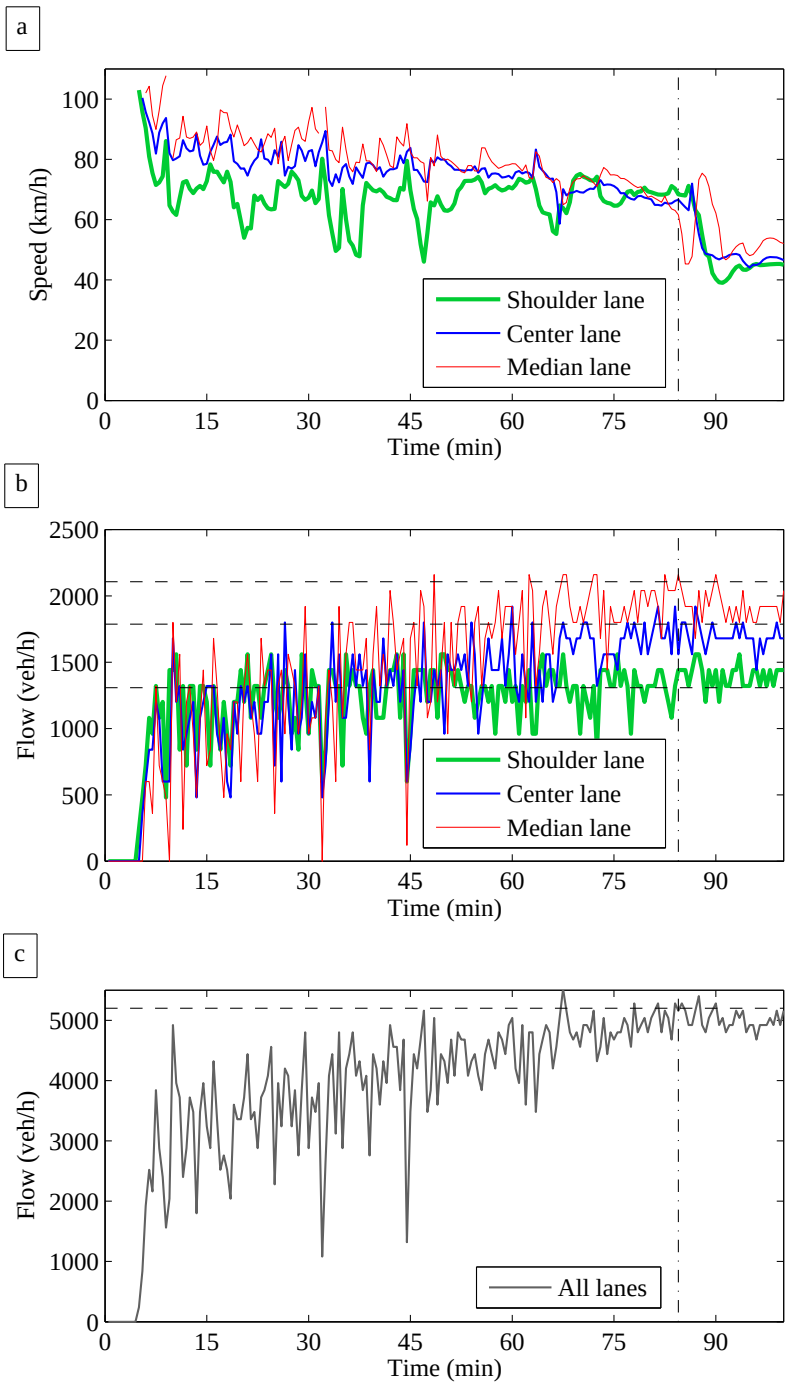

Figure 3. Speeds and flows over time at location x = 8.2 km (i.e., near the end of the sag vertical curve) in the base scenario (first simulation replication). The dash-dotted lines show the time-to-breakdown (TTBD). The dashed lines show the average demand after t = 75 min.

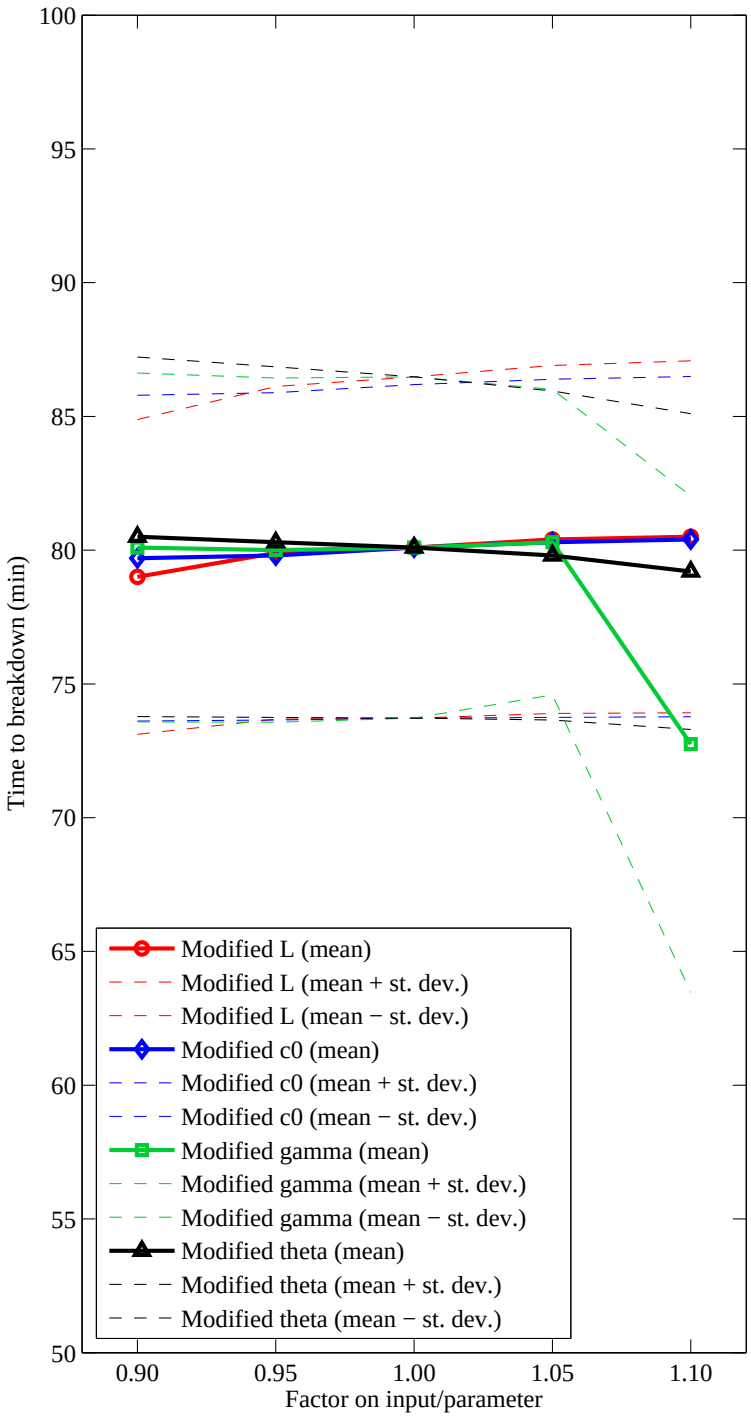

Figure 4. Sensitivity analysis: time-to-breakdown in each scenario (mean and mean plus/minus one standard deviation of five simulation replications).

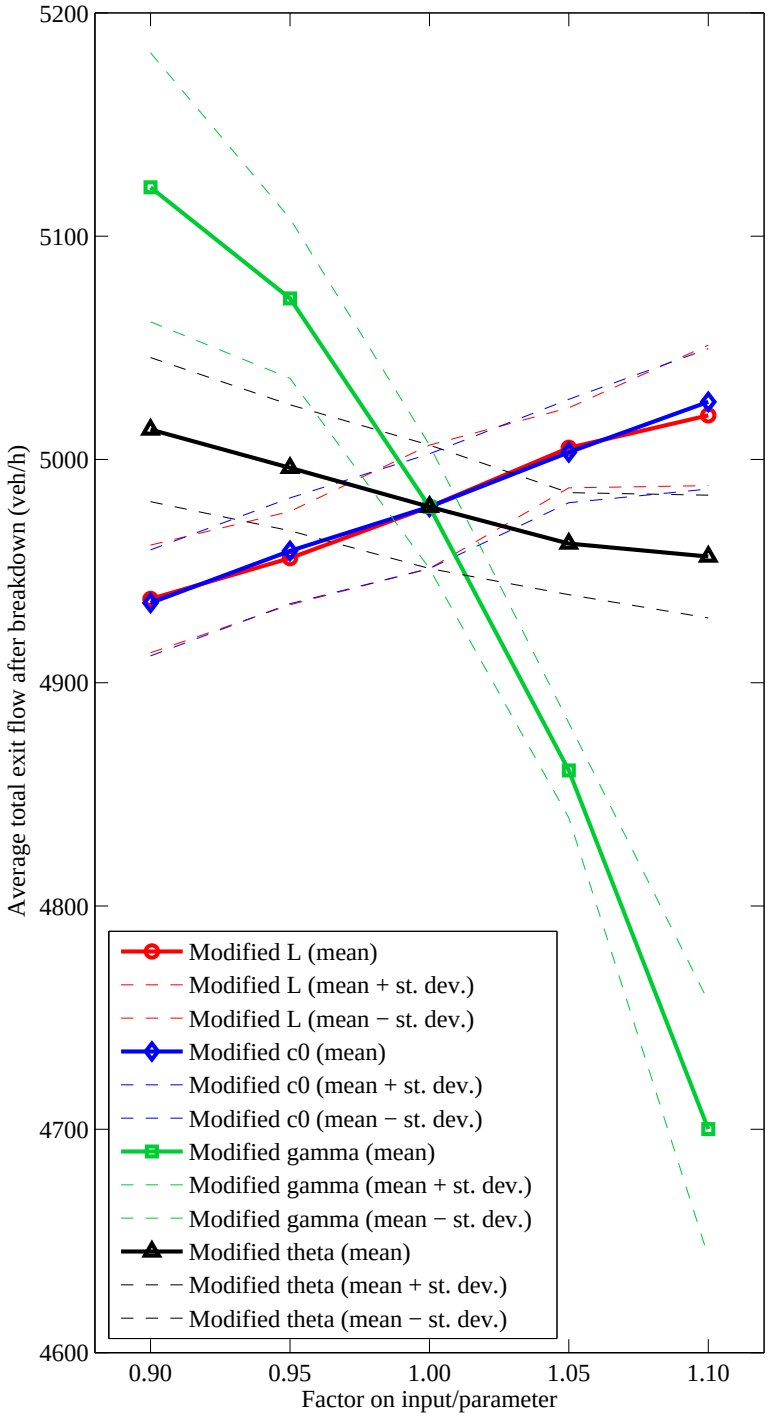

Figure 5. Sensitivity analysis: average total exit flow after breakdown in each scenario (mean and mean plus/minus one standard deviation of five simulation replications).

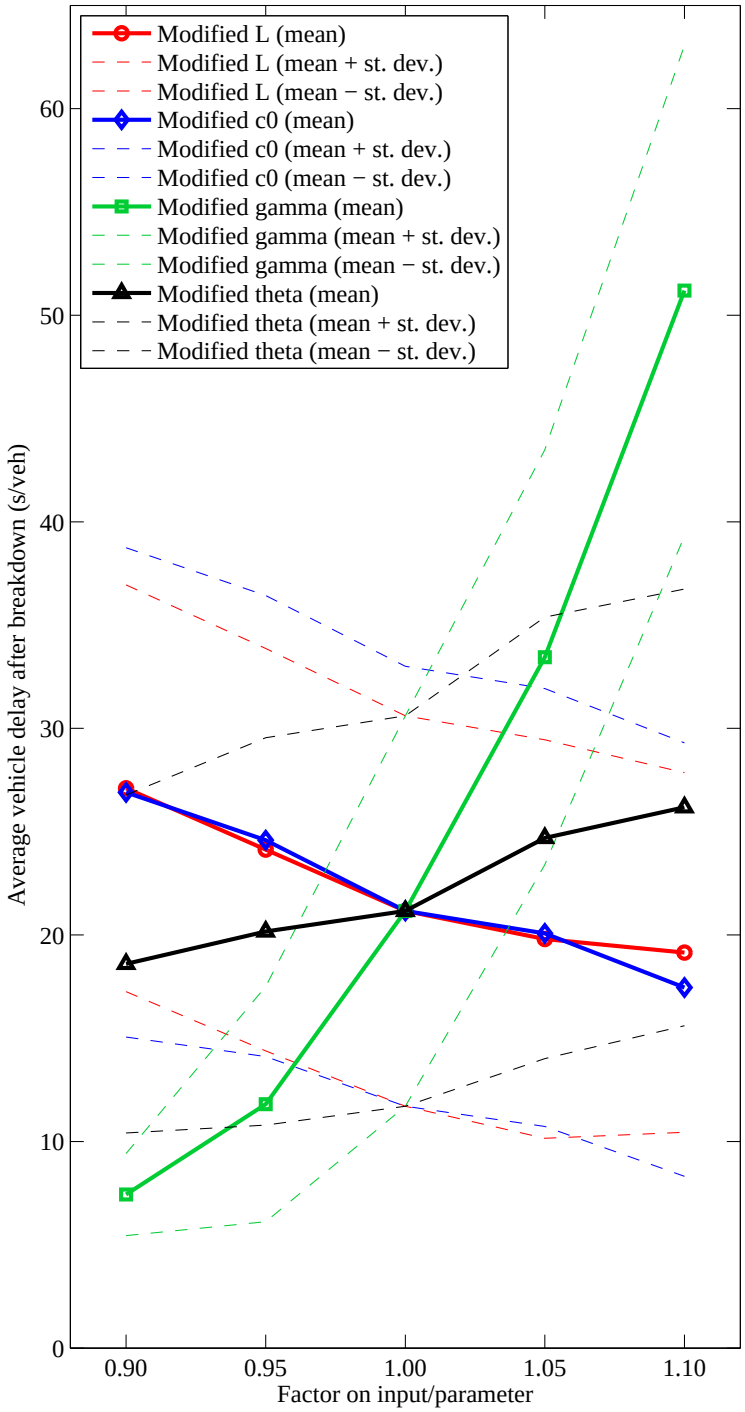

Figure 6. Sensitivity analysis: average vehicle delay after breakdown in each scenario (mean and mean plus/minus one standard deviation of five simulation replications).

Table 1. Parameters of the car-following model and the lane change model (base scenario).

Vehicle type	Car			Truck
Driver type	Car driver 1	Car driver 2	Car driver 3	Truck driver
a_0 (m/s^2)	1.25	1.25	1.25	0.50
b_0 (m/s^2)	1.80	1.80	1.80	1.50
$T_{F,0}$ (s)	1.45	1.20	1.15	1.50
s_s (m)	3	3	3	3
$v_{des,0}$ (km/h)	100	100	100	
v_{crit} (km/h)	60	60	60	60
c_0 (s^{-1})	0.00042	0.00042	0.00042	0.00042
θ (m/s^2)	9.81	9.81	9.81	9.81
γ (-)	1.15	1.15	1.15	1.15
δ^*(-)	0.92	0.97	1.03	1.00
σ_δ (-)	0.03	0.10	0.10	0.00
$v^*_{des,t}$ (km/h)				85
$\sigma_{vdes,t}$ (km/h)				2.5
$T_{min,0}$ (s)	0.56	0.56	0.56	0.56
τ (s)	25	25	25	25
x_0 (m)	200	200	200	200
v_{gain} (km/h)	70	50	50	70
d^{ij}_{free} (-)	0.365	0.365	0.365	0.365
d^{ij}_{sync} (-)	0.577	0.577	0.577	0.577
d^{ij}_{coop} (-)	0.788	0.788	0.788	0.788

Table 2. Traffic composition.

Vehicle type	Car	Car	Car	Truck
Driver type	Car driver 1	Car driver 2	Car driver 3	Truck driver
Shoulder lane	90%	0%	0%	10%
Center lane	0%	95%	0%	5%
Median lane	0%	0%	100%	0%

Table 3. Sensitivity analysis: model inputs in each scenario.

	L (m)	c_0 (s^{-1})	γ(-)	θ (m/s^2)
Base scenario	600	0.00042	1.15	9.81
Scenarios with modified L	0.90 · 600	0.00042	1.15	9.81
	0.95 · 600	0.00042	1.15	9.81
	1.05 · 600	0.00042	1.15	9.81
	1.10 · 600	0.00042	1.15	9.81
Scenarios with modified c_0	600	0.90 · 0.00042	1.15	9.81
	600	0.95 · 0.00042	1.15	9.81
	600	1.05 · 0.00042	1.15	9.81
	600	1.10 · 0.00042	1.15	9.81
Scenarios with modified γ	600	0.00042	0.90 · 1.15	9.81
	600	0.00042	0.95 · 1.15	9.81
	600	0.00042	1.05 · 1.15	9.81
	600	0.00042	1.10 · 1.15	9.81
Scenarios with modified θ	600	0.00042	1.15	0.90 · 9.81
	600	0.00042	1.15	0.95 · 9.81
	600	0.00042	1.15	1.05 · 9.81
	600	0.00042	1.15	1.10 · 9.81